УДК 539.172.8

AN EXPERIMENT TO SEARCH CUMULATIVE MUON PAIRS WITH LOW INVARIANT MASS

S.V.Afanasiev, Yu.S.Anisimov, S.N.Bazylev, J.Chmielewski, D.Enkhbold, O.P.Gavristhuk, I.G.Golutvina, V.I.Ilyushchenko, L.K.Ivanova, G.B.Khorsheva, A.N.Khrenov, V.S.Korolev, V.A.Kuznetsov, A.G.Litvinenko, A.I.Malakhov, P.K.Maniakov, E.N.Matveeva, G.L.Melkumov, D.P.Mikhalev, A.S.Nikiforov, A.N.Parfenov, V.G.Perevozchikov, T.D.Pilipenko, A.V.Piljar, S.G.Reznikov, O.G.Rubina, A.Yu.Semenov, A.E.Senner, N.A.Shutova, V.A.Smirnov, V.S.Stavinsky, V.A.Trofimov, V.V.Trofimov, D.V.Uralsky, P.I.Zarubin, I.Zborovsky, L.Ja.Zhiltsova
Joint Institute for Nuclear Research, Dubna

V.K.Bondarev
Leningrad University, USSR

N.Ghiordanescu
Bucharest University, Romania

M.Horoi, M.Pentia
Bucharest Institute for Physics and Nuclear Engineering, Romania

V.E.Kovtun
Kharkov University, USSR

W.Olejniczak
Łódź University, Poland

M.Pachr, M.Šumbera
Institute of Nuclear Physics, Řež near Prague, ČSFR

B.Słowinski
Warsaw University of Technology, Poland

Yu.I.Titov
Kharkov Physical Technical Institute, USSR

SPHERE Collaboration

Muon pair production with small invariant mass has been observed beyond the nucleon-nucleon kinematic limit. The obtained value of cross-section does not contradict a universal picture of the cumulative effect.

The investigation has been performed at the Laboratory of High Energies, JINR.

Эксперимент по поиску образования кумулятивных мюонных пар с малой инвариантной массой

С.В.Афанасьев и др.

Процесс рождения мюонных пар с малой инвариантной массой был зарегистрирован за кинематическим пределом нуклон-нуклонных соударений. Полученная величина сечения для этого процесса не противоречит ранее установленной универсальной картине кумулятивных процессов.

Работа выполнена в Лаборатории высоких энергий ОИЯИ.

Introduction

Dimuon production in hadron-nucleus and nucleus-nucleus collisions is a direct source of information about their internal structure. Besides, it makes possible to select a vector meson production signal by a lepton decay mode. The latter circumstance is of particular significance in relativistic nuclei collisions, where combinatorial background brings forth problems in resonance signal isolation by hadronic decay mode.

The program of research of the cumulative particle production in the framework of the SPHERE project [1] foresees studies of cumulative vector mesons. From the experimental point of view, a forward dipole magnet spectrometer of the setup SPHERE is apparently an optimum solution for the registration of muon pairs in a relatively narrow forward angle cone corresponding to the fragmentation of beam nucleus. The relativistic invariant scale variable or cumulative number X_{II} , used earlier for the description of cumulative production in the target fragmentation region [2], can be considered as a minimum target mass in units of the nucleon mass. Let us define X_I . For the beam fragmentation it corresponds to a beam particle momentum part needed to obey the 4-momentum conservation law for particle production with a given momentum and mass. In this case using lab. system variables, the expression X_I can be written as:

$$X_I = \frac{E_{\mu\mu} M_p - \frac{M_{\mu\mu}^2}{2}}{E_0 M_p - M_p^2 - (E_0 E_{\mu\mu} - P_0 P_{\mu\mu} \cos\theta)}, \qquad (1)$$

where E_0 and P_0 are the beam nucleus total energy and momentum per nucleon, respectively; M_p, the nucleon mass; $E_{\mu\mu}$, $P_{\mu\mu}$, $M_{\mu\mu}$ and θ, the total energy, momentum, mass and production angle of the cumulative particle, respectively. If the energies are much larger than the masses at a zero production angle, one can obtain a simple approximation of formula (1):

$$X_I \approx \frac{E_{\mu\mu}}{E_0}.$$

Figure 1 shows a relation between X_I and momentum $P_{\mu\mu}$ for the particle with mass $M_{\mu\mu}$=770 MeV/c^2 flying straightforward.

As established in the experiment [3], the inclusive spectra of cumulative particles can be described reasonably well with the function:

$$\frac{1}{A} E \frac{d\sigma}{d\vec{p}} = C \exp(-X/\langle X\rangle)\ \phi(p_t^2), \qquad (2)$$

where $\langle X\rangle = 0.12$ for deuteron fragmentation.

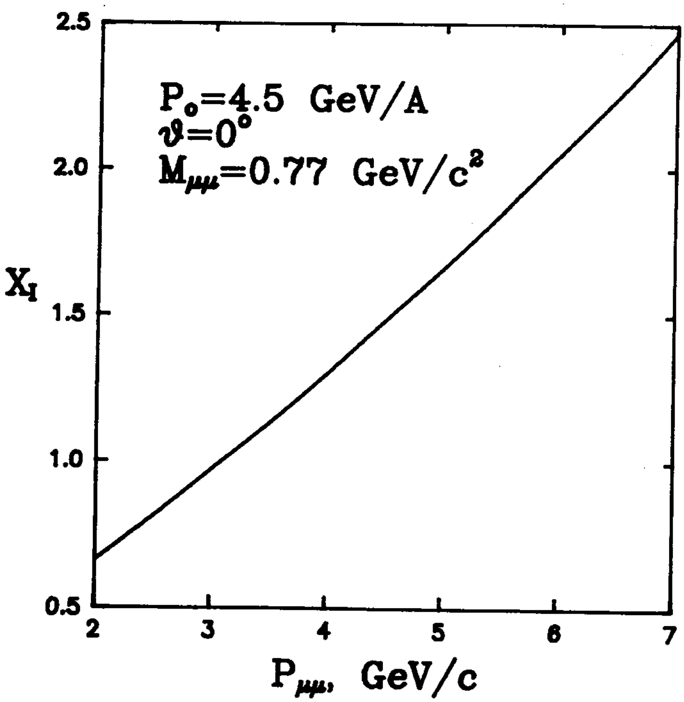

Fig.1.

To estimate the dimuon cross-section normalization parameter C, and to investigate the possibility of observing resonances near and beyond the nucleon-nucleon kinematic limit, we have made measurements of deuteron beam fragmentation into dimuons by the beam dump method. Electromagnetic losses of energy put restrictions on a minimum momentum of the muon penetrating through the absorber material. In addition, the absorber extinguishes a hadron-electromagnetic shower caused by the incoming deuteron. Such an approach permitted the muon pair production with large invariant mass to be measured down to very small cross-sections /4/. At the present time the absence of biological shielding around the SPHERE experimental area limits the value of admissible beam intensity. The beam dump method opens up a possibilities to gain greater luminosity.

Setup Description

Measurements were taken with a beam dump assembly using detectors intended for a forward part of the SPHERE spectrometer (see fig.2). The beam particles were 4.5 GeV/c per nucleon deuterons extracted from the Dubna Synchrophasotron with an intensity of about 10^6 per accelerator cycle. The lead target ($0.5 \times 0.5 \times 0.5$ m^3) served as a secondary hadron absorber. The beam was monitored by the telescope composed of three scintillation counters S1, S2 and S3 with the dimensions of $90 \times 90 \times 5$ mm^3, $120 \times 120 \times 10$ mm^3 and $50 \times 50 \times 3$ mm^3, respectively.

The muon pairs from the target were detected by scintillation hodoscopes H1-H4. The hodoscopes were interleaved with half a metre thick iron absorbers. Each hodoscope consists of three planes. The counters in the X-plane are oriented along the y-axis (vertical) while those in the Y-plane along the x-axis (horizontal). The U-plane which is needed to correlate X-plane hits with Y-plane ones, is rotated with respect to the horizontal axis by 20°. Each plane was assembled of twenty $1000 \times 40 \times 5$ mm^3 and six $440 \times 40 \times 5$ mm^3 scintillation bars. The hodoscope counters were made of polystyrene scintillator /5/. Each bar is viewed on one side through a plexiglass light guide by a FEU-85 photomultiplier. A 120×120 mm^2 hole was made in the center of each hodoscope plane.

A 56-cell Cherenkov matrix hodoscope was used to determine a muon intersection coordinate more precisely. Each hodoscope cell consisted of a $50 \times 50 \times 25$ mm^3 plexiglass Cherenkov light radiator and a FEU-85 photomultiplier.

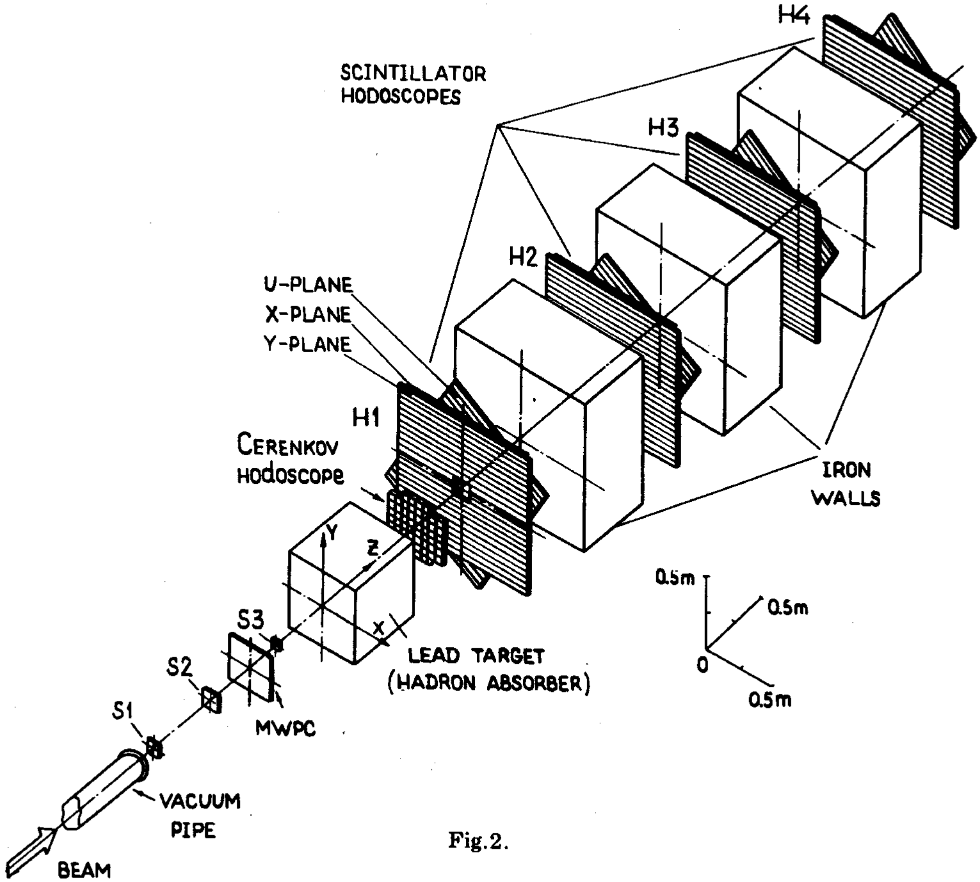

Fig.2.

Registration Efficiency and Background

The arrangement of the setup components and the thickness of the absorbers were optimized by means of GEANT3 program package [6] for the registration of cumulative muon pairs. Simulation included the distributions of inelastic deuteron vertices in a lead absorber and the momenta of muons produced by decay of a particle with mass $M_{\mu\mu}$, longitudinal and transverse momentum P_z and P_t, corresponding to $X_I > 1$ (see fig.1). Some 10^3 decays were generated for each desirable combination of $M_{\mu\mu}$, P_z and P_t. The trajectories of muons were calculated up to the exit of tracks from the working volume or to stopping points inside it. Electromagnetic losses of energy and multiple scattering were taken into account. The pairs penetrating beyond planes H1-H4 and missing the central hole in H1 were selected. The requirement for opposite signs of muon coordinates in the X-Y projection gave an additional constraint to be essential for decays with nonzero P_t.

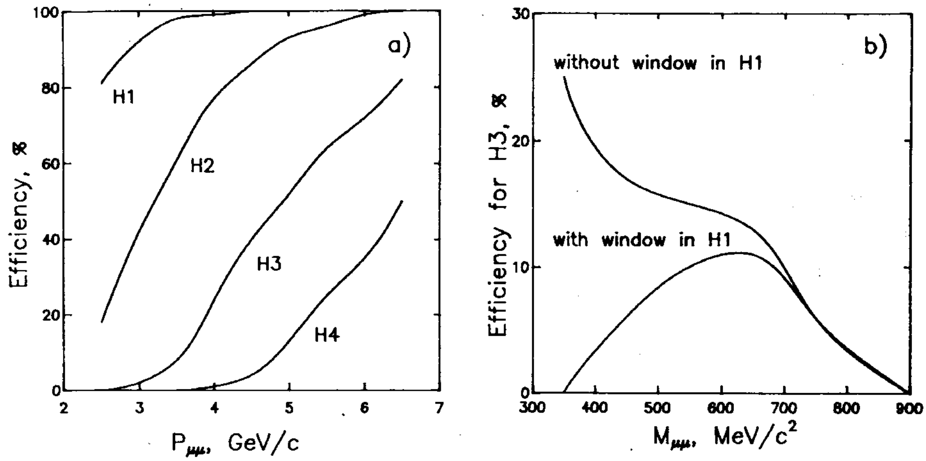

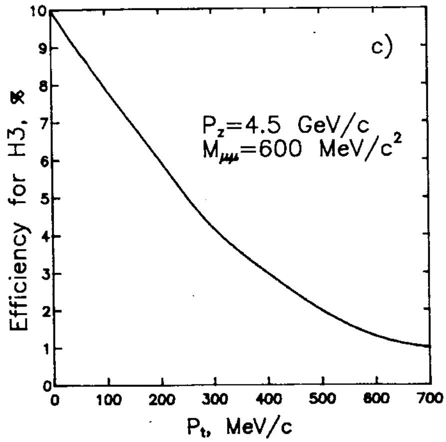

Fig.3.

We defined the registration efficiency as the number of events satisfying the described conditions divided by the total number of generated pairs at given $M_{\mu\mu}$, P_z and P_t. Figure 3 shows the efficiency as a function of these parameters. The penetration efficiency curve for the forward production of mass $M_{\mu\mu}$ = 250 MeV/c^2 is presented in fig.3a. The comparison with fig.2 shows a highly effective selection of muons within the cumulative region by hodoscopes H3 and H4. The efficiency smoothly decreases with increasing the pair mass (fig.3b, upper curve). The central hole in H1 changes significantly the shape of this curve (fig.3b, lower curve). The shape of the P_t-dependence is presented in fig.3c for $M_{\mu\mu}$ = 600 MeV/c^2 corresponding to a maximum in fig.3b.

Besides, it was necessary to estimate the fraction of noninteracting pion pairs, muons from pion decays and their combination. For the first time such a background was estimated in the experiment [7], devoted to the measurement of muon pair photoproduction. Stopping power method was used to determine the muon energy and to suppress the hadron flux. The dimensions of setup [7] were approximately the same as ours. The total background was 14%.

On generating the passage of 10^5 pions with a momentum of 2 GeV/c, only 97 pions and 139 decay muons have passed up to H3. Thus, penetration probability is about $3 \cdot 10^{-3}$. The ratio of the decay branching $(\rho^\circ \to \mu^+\mu^-)/(\rho^\circ \to \pi^+\pi^-)$ is equal to $7.3 \cdot 10^{-4}$. This gives the background at a level of 8%.

For analytical calculations of these background processes, the π pair production cross-section was assumed to be 10^4 times larger than the cross-section for μ pair production. The inelastic cross-section for pion collisions with Pb and Fe were taken from paper [9]. From our calculation the background percentage as compared to the μ pair rate is:

$W(\pi, \pi) = 2\%$ $\quad W(\pi, \mu) = 6\%$ $\quad W(\mu, \mu) = 5\%$.

Both estimates are in more or less good agreement.

Double nuclear scattering makes an additional contribution. Muon pair production in the secondary interaction process is due to the following chain:

$$D + Pb \to P + X_1$$
$$\hookrightarrow P + Pb \to \mu^+\mu^- + X_2,$$

where X_1 and X_2 are any other products of the reactions, P denotes the secondary nucleon producing μ pair in collision with lead nucleus. The proton momentum has to be greater than or equal to the incident deuteron momentum per nucleon because the cumulative scale variable X, for detecting μ pairs, approximately equals 1. For this kinematic region the deuteron fragmentation cross-sections on ^1H, ^1D and ^{12}C, were measured in experiments [10,11]. The cross-section on lead was obtained from extrapolation of these data assuming an $A^{2/3}$ dependence. The muon pair production cross-section in secondary interactions, was brought out from ref. [12]. Consequently, the double nuclear scattering background compared to the μ pair rate is:

$W(D\,Pb \to P\,Pb \to \mu\mu) = 6\%$.

Thus, the total background for muon pair registration, does not exceed:

$W \leq 19\%$.

Trigger and Data Acquisition

Figure 4 shows a logic diagram of the trigger and data acquisition systems. To achieve the goal of triggering on dimuon events and reducing the background to a minimum while keeping a reasonable length of cable

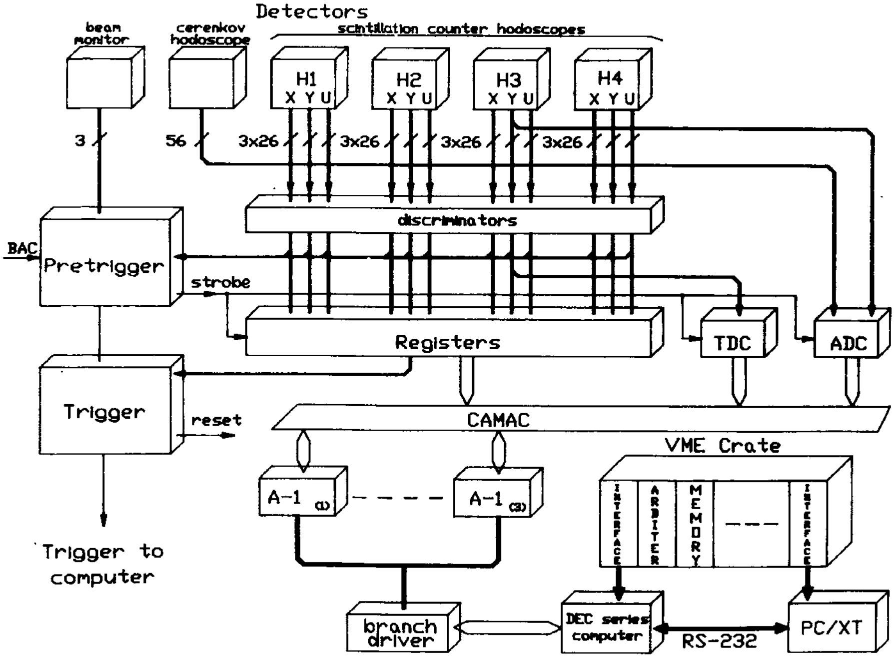

Detectors
beam monitor
cerenkov hodoscope
scintillation counter hodoscopes
H1 X Y U
H2 X Y U
H3 X Y U
H4 X Y U
3
56
3x26
3x26
3x26
3x26
discriminators
BAC
Pretrigger
strobe
Registers
TDC
ADC
Trigger
reset
CAMAC
VME Crate
A-1
A-1
INTERFACE
ARBITER
MEMORY
INTERFACE
Trigger to computer
branch driver
DEC series computer
RS-232
PC/XT

Fig.4.

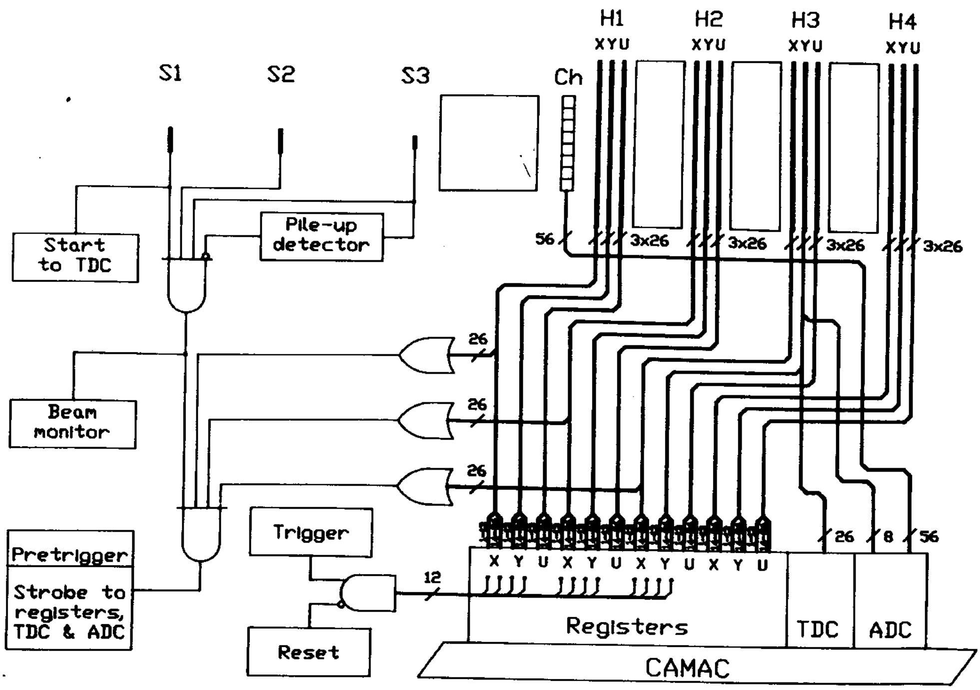

H1 XYU
H2 XYU
H3 XYU
H4 XYU
S1
S2
S3
Ch
Start to TDC
Pile-up detector
56
3x26
3x26
3x26
3x26
26
26
26
Beam monitor
Pretrigger
Strobe to registers, TDC & ADC
Trigger
Reset
12
26
8
56
X Y U X Y U X Y U X Y U
Registers
TDC
ADC
CAMAC

Fig.5.

delays, the trigger decision is made at two levels with stepwise decreasing rates.

A flow chart of the trigger logic is shown in more detail in fig.5. The first level trigger (pretrigger) is provided by the coincidence of a beam monitor signal and 3 OR signals from the X-planes of hodoscopes H1-H3. In turn, the beam monitor signal is caused by the coincidence of 3 signals from the monitor scintillation counters vetoed by a beam particle pile-up detection circuit with 35 ns resolution time. This ensures at least one charged particle to pass through the first three hodoscopes and to be uniquely related in time to a single beam particle.

The second level trigger uses signals from the fast logical OR outputs of the latches of the hodoscopes' counters (coincidence registers). A positive trigger decision is issued in the case of coincidence of 12 OR signals from each half of the X and Y-planes of hodoscopes H1-H3. Thus, the requirement on a passage of at least two particles having some degree of scattering symmetry is realized.

The typical beam intensity was $\simeq 10^6$ per spill, the pile-up detector rate $\approx 2 \cdot 10^5$, the pretrigger rate ≈ 800 and a trigger rate, 0.1. The total rates of hodoscopes H1, H2 and H3 were 10^6, $5 \cdot 10^5$ and $5 \cdot 10^4$, respectively.

The hodoscope planes provide coordinate information. In addition, analog and time information is read out from each counter of the H3 hodoscope Y-plane. For time measurements a common "start" signal is provided by beam counter S3; each counter of this plane issues a "stop" signal for its TDC channel. All data are recorded in the latches, ADCs and TDCs by a pretrigger induced strobe. The strobe duration for the latches is about 60 ns. A positive decision on the second level trigger initiates a data readout procedure. Readout is performed by a CAMAC branch driver /8/ with three A-1 crate controllers via a direct memory access channel into an on-line computer. The time needed for acquisition of one event of a 238 byte length is about 0.8 ms. In the case of a negative decision the trigger logic generates a fast reset signal for CAMAC modules. The deadtime for such an event does not exceed 2 μs .

Data acquisition is performed by two computers: Elektronika-60 (LSI-11 compatible) and IBM PC/XT. Elektronika-60 directly connected to the CAMAC branch acquires data event by event into a memory buffer during a spill. The data are transferred to IBM PC/XT via a VME memory module between accelerator cycles. To interchange control words and messages, the computers are interconnected by means of a standard serial interface RS-232C. This interface can be also used as an auxiliary channel for data transfer. IBM PC/XT writes data on a hard disk, books, displays histograms, displays event topology and performs overall control of the experiment.

Data Analysis and Event Identification

A total statistics of 9217 events triggered as described above was recorded during a two-week run. This corresponds to $4.0 \cdot 10^{10}$ deuterons passed towards the target.

Events which do not contradict the hypothesis of passage of two charged particles through at least the first three hodoscopes were picked out by stepwise application of the selection criteria. Such an approach allows one to estimate the upper and lower limits of the effect cross-section under the conditions of poor track-finding possibilities. Because of strong influence of multiple scattering, we decided to apply the following cuts:

— the number of signals from each plane of hodoscope H1 should be less than 7, H2 — less than 6 and H3 — less than 5;

— the number of resolved hits at each hodoscope should be greater than 1 and less than 5; a hit was assumed as "resolved" in the case of three-fold X, Y, U crossing or two-fold X, Y crossing at the areas not covered by the U-planes;

— all hits at the first hodoscope should be located in the central square with a 40 cm side;

— there should be at least two hits at each hodoscope with opposite sign coordinates.

The first and third cuts suppress the hadronic shower contribution, the second one suppresses the contribution of a neutron flux and the fourth one affirms a trigger condition for these hits. The analysis of the time spectra has shown a negligible contribution of accidentals. All the above criteria were satisfied by 43 events. This number was taken as a basis to estimate the upper limit of the cross-section.

At the second stage these events were passed through the track finding procedure and visual analysis of the longitudinal and transverse projections of the hits in the hodoscopes; 5 candidates in "good" dimuon events were picked out. Figure 6 shows a longitudinal projection of one of these events. They served as a basis for estimating the lower limit. In other words, we have determined limits on the dimuon yield within the covered kinematic region.

Fig.6.

Cross-Section Estimation

The goal of the experiment was to measure the integral muon pair production cross-section within the covered angle, momentum and effective mass regions. The C parameter can be estimated, assuming cross-section parametrization (2). The formula for muon pair yield may be written as:

$$N_{\mu\mu} = I_d N_A \frac{1}{A_t} P_t \int_0^L \exp(-a_{in}\ell)\, d\ell \int \frac{p^2}{E}\, dp \int dM \int d(\cos\theta) \int d\phi \times$$
$$\times\, \epsilon(\ell, p, M, \cos\theta)\, E \frac{d\sigma}{d\vec{p}\, dM}, \qquad (3)$$

where I_d is the total deuteron flux; N_A, Avogadro number; ρ_t, A_t and L, the density, atomic number and thickness of the target, respectively; ϵ, the efficiency for the μ pair registration; a_{in}, the inverse nuclear inelastic length of deuterons in lead; θ and ϕ, polar and azimuthal angles, respectively; $E d\sigma / d\vec{p}\, dM$, the invariant cross-section for μ pair production.

We suppose that the cross-section parametrization is similar to that used in cumulative particle production [13]:

$$E\frac{d\sigma}{d\vec{p}\,dM} = C_{\mu\mu}\cdot\exp(-X/\langle X\rangle)\cdot\phi(p_t^2)\cdot f(M_{\mu\mu}).$$

The transverse momentum dependence $\phi(p_t^2)$ is assumed to be the same as that for cumulative pion production:

$$\phi(p_t^2) = 0.9\cdot\exp(-2.7\cdot p_t^2) + 0.1.$$

The mass dependence $f(M_{\mu\mu})$ contains the Breit — Winger mass distribution of the ρ-meson and a constant continuum:

$$f(M_{\mu\mu}) = \frac{\Gamma_\rho}{2\pi}\cdot\frac{1}{(M_{\mu\mu}-M_\rho)^2+\Gamma_\rho^2/4} + \frac{2\delta}{\pi\Gamma_\rho},$$

where M_ρ and Γ_ρ are the mass and the width of the ρ-meson, respectively, δ, the ratio of continuum to ρ-meson signal for $M_{\mu\mu} = M_\rho$.

Integrating expression (3), we derive a relation between the experimentally observed values $N_{\mu\mu}$ and I_d:

$$N_{\mu\mu} = 0.6\cdot C_{\mu\mu}\delta\cdot 10^{-10} I_d.$$

Using the total deuteron flux, the upper and lower limits of the registered muon pairs, we obtain:

$$C_{\mu\mu}\delta = (2.1 \div 21)\ \text{mb}\cdot\text{GeV}^{-2}c^3.$$

After integration over the covered mass region, the upper and lower limits of the muon pair production cross-section are equal to:

X	0.9	1.0	1.2
$E\frac{d\sigma}{d\vec{p}}\left(\frac{\text{mb}}{\text{GeV}^2/c^3}\right)$	$(1.2\div12)\cdot10^{-3}$	$(5.0\div50)\cdot10^{-4}$	$(9.5\div95)\cdot10^{-5}$

To compare this with the cross-section of cumulative pion production, we have to extrapolate the known data [3] on proton-deuteron collisions. Assuming the $A^{2/3}$ dependence of the deuteron fragmentation cross-section into cumulative pions, we obtain its value for lead. This gives us, for the same cumulative number X, a reasonable relation:

$$(E \cdot d\sigma/d\vec{p})_{\mu\mu} \simeq (E \cdot d\sigma/d\vec{p})_{\pi} \cdot 10^{-4}.$$

Conclusions

We have searched for the deuteron fragmentation into cumulative muon pairs with small invariant mass. Our result can be summarized as follows: the muon pair production beyound the kinematic limit of nucleon-nucleon collisions has been observed. The cross-section estimate does not contradict the previously established picture of the universality of cumulative production. The obtained results could serve as a starting point for experiments to be planned in this field.

References

1. Averichev S.A. et al. — JINR Communication, P1-85-512, Dubna, 1985.
   Averichev G.S. et al. — In: Proceedings of the Third International Symposium "Pion-Nucleon and Nucleon-Nucleon Interactions", vol.2, p.357, Gatchina, USSR, 1989.
2. Baldin A.M., Panebratsev Ju.A., Stavinsky V.S. — Doklady Academii Nauk SSSR (USSR Academy of Sciences Reports), vol.279, p.1352, 1984.
3. Baldin A.M. et al. — JINR, E1-82-472, Dubna, 1982.
4. Christenson J.H. et al. — Phys. Rev. Lett., 1970, 25, p.1523.
5. Ammosov V.V. et al. — JINR preprint, 13-88-779, Dubna, 1988.
6. Brun R. et al. — GEANT3, CERN, DD/EE/84-1, September, 1987.
7. De Pagter J.K. et al. — Phys. Rev. Lett., 1964, 12, p.739.
   Boyarski A.M. et al. — Phys. Rev. Lett., 1966, 16, p.35.
8. Smirnov V.A. et al. — JINR Communication, 10-81-528, Dubna, 1981.
9. Barashenkov V.S. — JINR Communication, P2-90-257, Dubna, 1990.
10. Zaporozhets S.A. et al. — In: Proceedings of the VIII International Seminar on High Energy Physics Problems, D1,2-86-668, vol.1, p.341, Dubna, 1987.
11. Azhgirei L.S. et al. — ibid., p.334, Dubna, 1987.
12. Kinoshita K. et al. — Phys. Rev. D, 1978, v.D17, p.1837-1840.
13. Stavinsky V.S. — JINR Communication, P2-9528, Dubna, 1976.

Received on November 16, 1990.